

Ferrocenyl Ligands

1,1'-Bis(pyrazol-4-yl)ferrocenes: Potential Clip Ligands and Their Supramolecular Structures

Mattia Veronelli,^[a] Sebastian Dechert,^[a] Anne Schober,^[a] Serhiy Demeshko,^[a] and Franc Meyer*^[a]

Abstract: Two ferrocene derivatives with pyrazoles appended at their C-4 position to both cyclopentadienyl (Cp) rings have been synthesized, namely, 1,1'-bis(1*H*-pyrazol-4-yl)ferrocene (H_2^{HL}) and 1,1'-bis(3,5-dimethyl-1*H*-pyrazol-4-yl)ferrocene (H_2^{MeL}). In the solid state, these are shown crystallographically to form supramolecular aggregates through intermolecular NH...N hydrogen bonds in either a dimeric (H_2^{HL}) or trimeric (H_2^{MeL}) arrangement. Variable-temperature NMR spectroscopy and diffusion-ordered spectroscopy (DOSY) evidenced the presence of $[H_2^{MeL}]_3$ trimers in $[D_8]$ toluene solution, whereas both H_2^{HL} and H_2^{MeL} exist as monomers in deuterated *N,N*-dimethylformamide ($[D_7]$ DMF) even at low temperatures. The kinetic pa-

rameters for the NH tautomerism have been determined. In their dianionic forms, both of these hybrid ferrocene/pyrazole molecules serve as ligands towards Cu^I , Ag^I , and Au^I ions. Matrix-assisted laser desorption/ionization mass spectrometry (MALDI MS) revealed the formation of $[M_2^{RL}]_3$ hexametallallic complexes, the structures of which are suggested to have D_{3h} symmetry with two metallomacrocyclic $[M(\mu-pz)]_3$ (pz = pyrazolate) decks connected by three ferrocene clips. Mössbauer spectra and preliminary luminescence data were collected for the proligands and the resulting complexes. Owing to the insolubility of the coinage-metal complexes, the electrochemical properties could be measured only for the two H_2^{RL} proligands.

Introduction

Pyrazoles and pyrazolates hold a prominent position as ligands in coordination chemistry, and their complexes with monovalent coinage metals (Cu^I , Ag^I , and Au^I) have attracted widespread interest.^[1] In combination with these monovalent metal ions, the pyrazolate anion $[pz]^-$ forms compounds with structures that range from polymeric chains^[2] to oligonuclear metallomacrocycles of different nuclearities. In the latter group, the planar trimeric ring $[M(\mu-pz)]_3$ is by far the most recurrent motif,^[1,3] though different examples of tetrameric and hexameric species have also been reported.^[1b,3,4] The structure adopted by each complex is dependent on the metal ion,^[3] the substituents at the heterocycle,^[3] and, in some cases, also on the specific synthetic and crystallization procedures.^[4a,4b,5] A second aspect of interest is the ability of pyrazolate coinage-metal complexes $[M(\mu-pz)]_n$ to act as supramolecular synthons. Intermolecular $d^{10}-d^{10}$ interactions usually lead to the formation of ordered supramolecular aggregates of polymeric $[M(\mu-pz)]_\infty$ ^[2,6] or trimeric $[M(\mu-pz)]_3$ units in the solid state.^[7] If the electronic characteristics of the ligands are changed, these complexes can act either as π -acids or π -bases,^[7c] and several supramolecular adducts with aromatic molecules^[7c,7d,8] or metal-based Lewis acids^[9] have been reported. Moreover, intra- and intermolecular

metallophilic contacts are the main factors responsible for the fascinating luminescence properties associated with this class of compounds.^[3,7a-7c,9a,10] In the past few years, different studies have focused on the possibility to obtain coinage-metal complexes with enhanced metallophilic contacts through the targeted design of ligands.^[11] Recently, we introduced the use of 1,1'-bis(pyrazol-3-yl)ferrocene molecules (H_2^{RL} ; Figure 1) as ligands towards Cu^I and Ag^I ions.^[12] The resulting hexametallallic species are characterized by two decks of M_3N_6 metallomacrocycles, which are forced to adopt an eclipsed conformation, because the ferrocene (Fc) units act as clips. Furthermore, the proligands H_2^{RL} themselves form hydrogen-bonded supramolecular structures in the solid state and in solution.

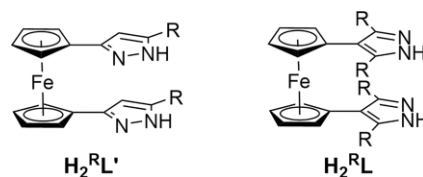


Figure 1. Representations of the pyrazole-substituted ferrocene frameworks with the heterocycles attached at the 3-position ($H_2^{RL'}$, left)^[12] and at the 4-position (H_2^{RL} , right); R = general substituent.

Ferrocene-based molecules have been investigated widely, and numerous ferrocene derivatives with N-heterocyclic substituents have been reported.^[13] These compounds have been used as ligands towards various metal ions^[13] or have been designed to form supramolecular structures through hydrogen bonds.^[14] Quite surprisingly, despite the well-established chemistry of both ferrocenes and pyrazoles, examples of hybrid mol-

[a] Institut für Anorganische Chemie, Georg-August-Universität Göttingen, Tammannstrasse 4, 37077 Göttingen, Germany
E-mail: franc.meyer@chemie.uni-goettingen.de
<http://www.meyer.chemie.uni-goettingen.de>

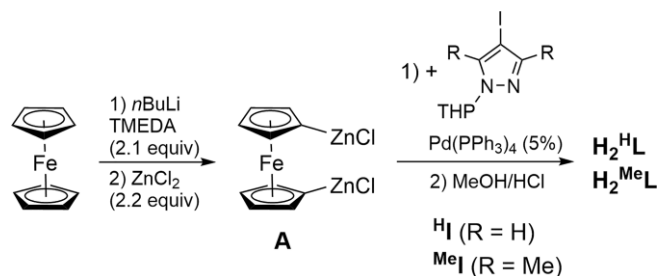
Supporting information and ORCID(s) from the author(s) for this article are available on the WWW under <http://dx.doi.org/10.1002/ejic.201600644>.

ecules composed of one ferrocene unit and two appended pyrazole rings are still very rare.^[12,15] Moreover, in all of these compounds, the metallocene is connected to the 3- or 5-position of the heterocycle, and examples of connectivity through the pyrazole C-4 atom are limited to monosubstitution.^[14c,16] In the present work, we fill this gap with the report of two distinct 1,1'-bis(pyrazol-4-yl)ferrocenes (H_2^{RL} ; Figure 1), namely, 1,1'-bis(1*H*-pyrazol-4-yl)ferrocene (H_2^{HL}) and 1,1'-bis(3,5-dimethyl-1*H*-pyrazol-4-yl)ferrocene (H_2^{MeL}). These proligands were characterized both in the solid state (X-ray diffraction and Mössbauer spectroscopy) and in solution (NMR spectroscopy and cyclic voltammetry). Furthermore, their potential use as ligands towards monovalent Cu^I, Ag^I, and Au^I ions was tested, and the resulting complexes were identified by mass spectrometry.

Results and Discussion

Proligands

The syntheses of the two proligands H_2^{HL} and H_2^{MeL} are based on a Negishi coupling protocol and were inspired by the procedure developed by Mochida et al. for 4-ferrocenyl-1-tritylpyrazole.^[14c] Ferrocene was deprotonated twice at the 1- and 1'-positions by the *n*BuLi/tetramethylethylenediamine (*n*BuLi/TMEDA) system (Scheme 1), and the subsequent addition of ZnCl₂ led to the formation of dizincated ferrocene **A**. Cross-coupling between this species and the appropriate tetrahydropyran-protected (THP-protected) 4-iodopyrazole [4-iodo-1-(tetrahydropyran-2-yl)-1*H*-pyrazole (**H^I**) or 4-iodo-3,5-dimethyl-1-(tetrahydropyran-2-yl)-1*H*-pyrazole (**H^{MeI}**)] was conducted in the presence of Pd(PPh₃)₄ (5 mol-% with respect to the starting ferrocene). After the workup of the reaction mixture and acidic deprotection of the pyrazole NH moieties, the target products were isolated in overall yields of 41 % (H_2^{HL}) and 32 % (H_2^{MeL}).



Scheme 1. Synthetic pathway for the proligands H_2^{HL} and H_2^{MeL} .

Both proligands were successfully crystallized, and their molecular structures were determined by X-ray diffraction. In both cases, a synperiplanar eclipsed conformation of the pyrazole moieties in the individual molecules was found (Figures 2 and S20–S21). The heterocycles are almost coplanar with the adjacent cyclopentadienyl (Cp) rings for H_2^{HL} (dihedral angles of 7.0° and 11.2°), whereas the interplanar angles are larger in H_2^{MeL} (they range from 17.6° to 23.0°; three independent molecules per unit cell), most likely because of the presence of steric hindrance between the Cp rings and the methyl substituents at the pyrazole ring. Remarkably, both molecules form supramolecular aggregates in the solid state through intermolec-

ular NH...N hydrogen bonds. H_2^{HL} crystallizes as a dimer (Figure 2, top) in which the four pyrazole units adopt a saddlelike disposition similar to those observed for common tetrameric pyrazoles.^[17] The same kind of arrangement was encountered recently in the solid-state structure of 1,1'-bis(5-methyl-1*H*-pyrazol-3-yl)ferrocene (H_2^{MeL} ; Figure 1).^[12] Consequently, each pyrazole ring of H_2^{HL} interacts with both heterocycles of a second molecule of H_2^{HL} , and the two ferrocenyl units point in two perpendicular directions to give a structure with crystallographic C₂ symmetry. Both possible enantiomers are found in the crystal structure, as the NH protons show a 1:1 disorder between the nitrogen atoms of the central belt of the dimer.

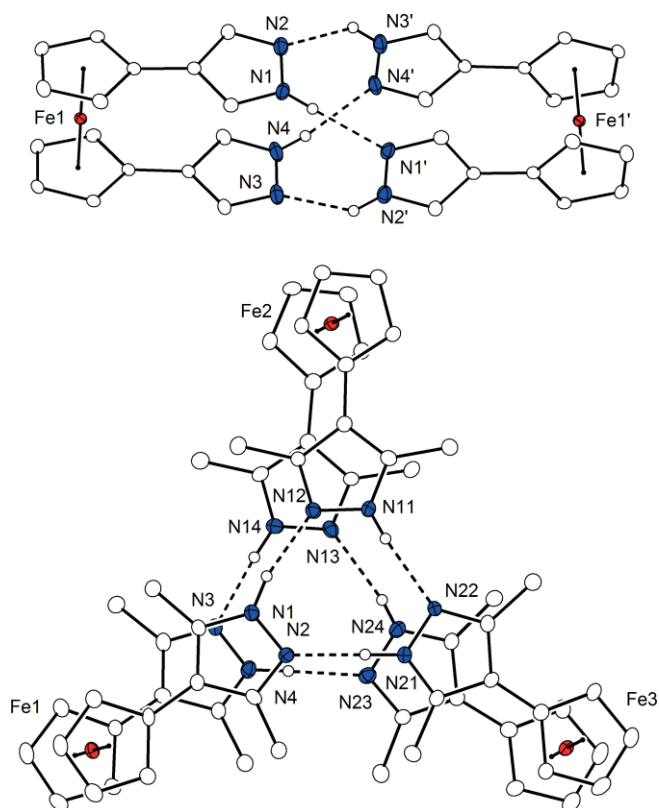


Figure 2. Supramolecular arrangements of H_2^{HL} (top) and H_2^{MeL} (bottom) in the solid state. The dashed lines emphasize intermolecular N–H...N hydrogen bonds.

In contrast, H_2^{MeL} crystallizes as a trimeric aggregate (Figure 2, bottom). The cyclic H-bonded arrangement of three pyrazole units found in each of the two decks of [H_2^{MeL}]₃ has been reported previously for several other pyrazoles.^[17a,17b] In the present case, two such (Hpz)₃ decks are stacked at a separation of ca. 3.73 Å because of the three ferrocene linkers that serve as clips. Only one tautomer of (H_2^{MeL})₃ was observed in the crystalline material, that is, the one in which the two pyrazole rings of the same H_2^{MeL} molecule have the protons on opposite nitrogen atoms. This results in a structure with an approximate (noncrystallographic) D₃ symmetry.

The stabilities of these supramolecular aggregates of H_2^{HL} and H_2^{MeL} in solution were investigated by NMR spectroscopy with the same (but deuterated) solvents employed for the crystallization process, that is, deuterated *N,N*-dimethylformamide

([D₇]DMF) and [D₈]toluene for H₂^HL and H₂^{Me}L, respectively. The ¹H NMR spectrum of H₂^HL at room temperature shows only four signals (two originating from the Cp protons, one from the 3-/5-H^{Pz} atoms, and one assigned to NH groups; see Figure S1, top), whereas a total of seven peaks would be expected if the structure found in the solid state was retained in solution. Thus, at room temperature, NH tautomerism and, most likely, rotation of the pyrazole rings around the bond linking them with the ferrocenyl moieties are operative. As the sample is cooled to temperatures below 240 K, the peak at $\delta \approx 7.6$ ppm (3-/5-H^{Pz}) splits into two resonances of equal integration (Figure S1); therefore, the NH tautomerism becomes slow on the NMR time scale. At the same temperature, the Cp protons remain pairwise equivalent, either because they are quite far from the pyrazole NH group and, thus, accidentally isochronous or because of the free rotation of the pyrazole rings along the 1-C^{Fc}/4-C^{Pz} bond that links the pyrazole and ferrocene subunits. Even at the lowest temperature limit of [D₇]DMF (223 K), H₂^HL exists as a monomer in solution, as ascertained by ¹H diffusion-ordered NMR spectroscopy (DOSY), which does not reveal any change of the volume of the proligand between 298 and 223 K (see below and the Supporting Information for details). The formation of a supramolecular aggregate of H₂^HL in solution is most likely prevented by the high polarity and the H-bond acceptor properties of the solvent [D₇]DMF. Unfortunately, NMR spectroscopy investigations in different media were not possible because of the insolubility of the proligand in solvents other than DMF and dimethyl sulfoxide (DMSO). By examining the temperature dependence of the signal of the 3-/5-H^{Pz} protons, the kinetic parameters associated with the NH...N tautomeric equilibrium were determined.^[18] From the coalescence temperature $T_c = 240$ K, the Gibbs activation energy was estimated to be 47.8 kJ mol⁻¹ (see the Supporting Information for details). The entropy and enthalpy of activation were derived by linewidth analysis, which gave $\Delta S^\ddagger = (-90.9 \pm 4.1)$ J K⁻¹ mol⁻¹ and $\Delta H^\ddagger = (26.7 \pm 1.06)$ kJ mol⁻¹ (Eyring plot shown in the Supporting Information). The derived activation energy is in line with the values reported for the tautomeric equilibrium of unsubstituted

pyrazole in hexamethylphosphoramide (HMPA: $\Delta G^\ddagger_{345} = 63$ kJ mol⁻¹)^[19] and DMSO ($\Delta G^\ddagger_{362} = 62$ kJ mol⁻¹,^[20] from the above parameters, the ΔG^\ddagger values for H₂^HL are calculated to be 58.1 and 59.6 kJ mol⁻¹ at 345 and 362 K, respectively). However, direct comparisons between different systems are difficult, because the pyrazole tautomerism is believed to proceed by multimolecular pathways rather than a unimolecular one^[17b] and is, thus, sensitive to solvent and concentration.^[17b] The negative value of ΔS^\ddagger for H₂^HL is also consistent with a multimolecular transition state.

The presence of trimeric [H₂^{Me}L]₃ species was detected in [D₈]toluene solution. By measuring the ¹H DOSY NMR spectra at 298 and 193 K and by using the residual protons of the solvent as an internal standard, it was demonstrated that H₂^{Me}L increases its volume by a factor of ca. 2.9 upon cooling (see Supporting Information for details). This value is in agreement, within experimental error, with the trimerization of H₂^{Me}L at low temperatures. As expected, the appearance of the ¹H NMR spectrum of H₂^{Me}L is temperature-dependent. At 298 K, the proligand exists in a monomeric form, and the NH tautomerism is fast on the NMR time scale; therefore, a highly symmetric molecule is detected (Figure 3, top). Below 270 K, the tautomerism becomes sufficiently slow that the three CH resonances of the spectrum each split into two resonances of equal integration; therefore, a total of seven signals can be seen at 213 K (at intermediate temperatures, some peaks originating from the Cp protons overlap and are difficult to distinguish; see Figure 3). These experiments indicate that the same kind of supramolecular aggregate is present in both the solid state and, at low temperatures, in solution. However, the NMR spectroscopy data did not permit us to determine the tautomeric form of the trimer in solution, which could have either D₃ or D_{3h} symmetry. NMR spectroscopy experiments also allowed us to estimate the Gibbs activation energy for the tautomeric equilibrium of the pyrazole moieties ($\Delta G^\ddagger \approx 54.2$ kJ mol⁻¹, $T_c \approx 270$ K for the CH₃ resonances; see the Supporting Information for details). The entropy and enthalpy of activation for the same process could not be determined, as the plot of $\ln(k/T)$ versus $1/T$ (Eyring plot; k

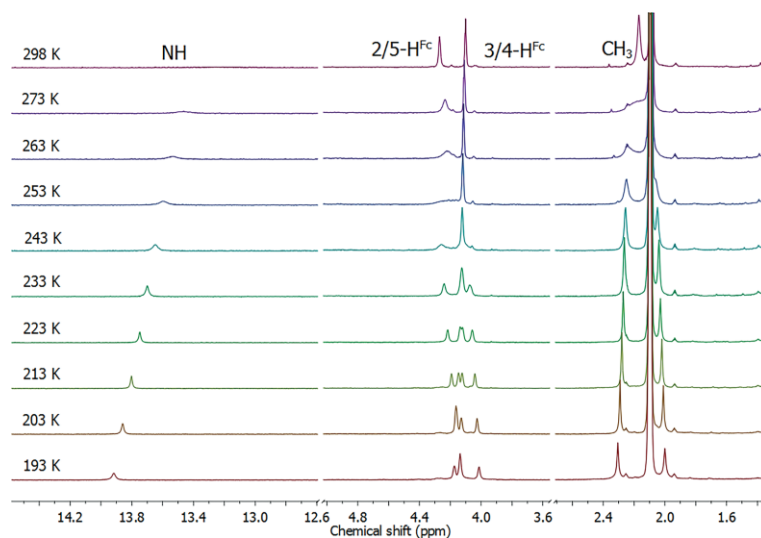


Figure 3. ¹H NMR spectra of H₂^{Me}L recorded in [D₈]toluene at different temperatures. The peak at $\delta = 2.08$ ppm is due to the residual protons of the solvent.

determined by linewidth analysis between 243 and 193 K) was not linear. This is, because the H_2^{MeL} system undergoes two distinct dynamic processes in the temperature range considered in the order of the NMR time scale, namely, NH tautomerism and aggregation to form the trimeric supramolecular aggregates. As expected, the formation of supramolecular structures of H_2^{MeL} in solution is sensitive to the solvent employed and can be prevented in more polar media capable of H-bonding. 1H DOSY NMR spectroscopy of H_2^{MeL} in $[D_7]DMF$ did not show any increase of the volume between 298 and 223 K, and the NH tautomerism also remained fast on the NMR time scale in this temperature range (Figure S2).

The electrochemical properties of both H_2^{HL} and H_2^{MeL} were investigated by cyclic voltammetry (CV) in $DMF/0.1\text{ M }[nBu_4N]PF_6$ solutions. Both compounds show an electrochemically reversible anodic process associated with the oxidation of the ferrocenyl moieties (linear dependence of the current on the square root of the scan rate; see Figures S5 and S6). The oxidation potential of H_2^{HL} is $E_{1/2} = -156\text{ mV}$ versus Fc/Fc^+ (Figure 4, left), whereas $E_{1/2}$ is -179 mV for H_2^{MeL} (Figure 4, right; the dependence of the peak separation ΔE_p on the scan rate ν is due to uncompensated solution resistance under the experimental conditions). The presence of two pyrazole units clearly renders the iron center of each proligand more electron-rich than that in the parent ferrocene and, thus, easier to oxidize. The slightly lower oxidation potential of H_2^{MeL} can be rationalized by the better electron-donating ability of the methyl substituents compared with that of the H-atoms present in H_2^{HL} . It is interesting to compare the oxidation potentials found for the two new proligands discussed here with that found for 1,1'-bis(5-methyl-1H-pyrazol-3-yl)ferrocene ($H_2^{MeL'}$; Figure 1), which we reported recently ($E_{1/2} = -50\text{ mV}$ in DMF).^[12] Despite the structural similarity of the systems, the oxidation of $H_2^{MeL'}$ is shifted anodically by more than 100 mV. Thus, the different connectivity of the pyrazole rings with the ferrocene moiety influences the electronic situation at the iron atom; the trends of the CV data are in line with the highest electron density of the pyrazole heterocycle at the 4-position.^[21]

To further characterize H_2^{HL} and H_2^{MeL} , their Mössbauer spectra were collected for solid material at 80 K. In both cases,

a single quadrupole doublet was observed with isomeric shifts and quadrupole splitting values typical for low-spin Fe^{II} and similar to those reported for ferrocene^[22] and 4-ferrocenyl-3,5-dimethylpyrazole.^[16a] As an example, the spectrum recorded for H_2^{HL} is shown in Figure 5, and Mössbauer parameters for proligands H_2^{MeL} and all coinage-metal complexes (see below) are listed in Table 1.

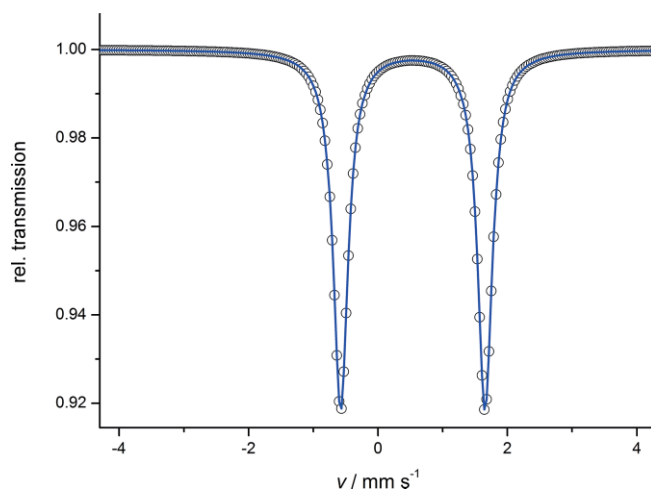


Figure 5. Mössbauer spectrum of solid H_2^{HL} at 80 K; the blue line represents a simulation with $\delta = 0.54\text{ mm s}^{-1}$ and quadrupole splitting $\Delta E_Q = 2.23\text{ mm s}^{-1}$.

Table 1. Mössbauer parameters [mm s^{-1}] of the two proligands H_2^{HL} and their complexes.

	δ	ΔE_Q
H_2^{HL}	0.54	2.23
H_2^{MeL}	0.55	2.37
$[Cu_2^{HL}]_3$	0.54	2.25
$[Cu_2^{MeL}]_3$	0.56	2.35
$[Ag_2^{HL}]_3$	0.55	2.24
$[Ag_2^{MeL}]_3$	0.56	2.36
$[Au_2^{HL}]_3$	0.54	2.28
$[Au_2^{MeL}]_3$	0.55	2.36
Ferrocene ^[22]	0.49	2.41

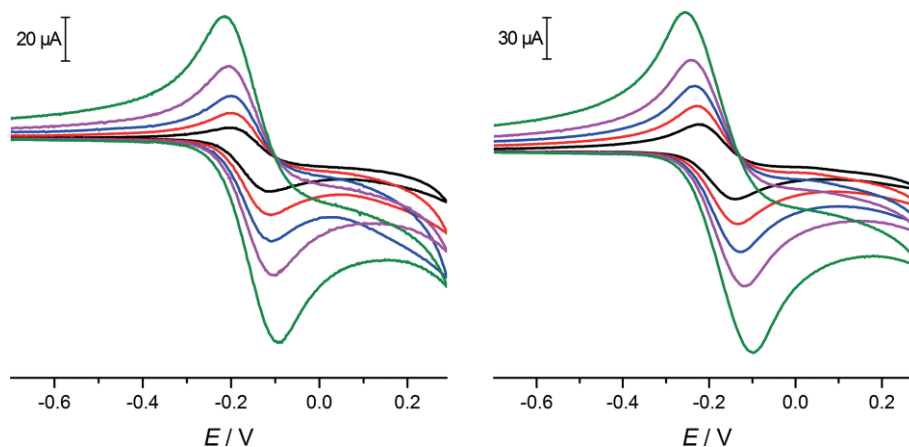


Figure 4. Cyclic voltammograms of H_2^{HL} (left) and H_2^{MeL} (right) in $DMF/0.1\text{ M }[nBu_4N]PF_6$ versus Fc/Fc^+ at different scan rates ($\nu = 20, 50, 100, 200, 500\text{ mV s}^{-1}$); $E_{1/2}(H_2^{HL}) = -156\text{ mV}$, $E_{1/2}(H_2^{MeL}) = -179\text{ mV}$.

Complexes

The two new hybrid ferrocene/pyrazole proligands H_2^HL and H_2^{MeL} were used, in their dianionic forms $[R^L]^{2-}$, as ligands towards monovalent Cu^I , Ag^I , and Au^I ions. The direct reactions of H_2^RL with 2 equiv. of the appropriate metal salt $\{[Cu(MeCN)_4][BF_4]$, $AgBF_4$, or $AuCl(SMe)_2$, respectively} in the presence of Et_3N led to the formation of compounds of general formula $[M_2^RL]_3$ ($M = Cu^I$, Ag^I , Au^I). With proligand H_2^{MeL} , the reactions were performed in MeOH for the copper complex and in MeCN for the Ag^I and Au^I salts to avoid any facile oxidation of the ferrocene unit (Fe^{II} to Fe^{III}) in the presence of the latter ions. The redox potential of the Ag/Ag^+ couple is highly solvent-dependent and reaches its minimum in MeCN ($E_{1/2} = 4$ mV vs. Fc/Fc^+).^[23] Owing to its lower solubility, H_2^HL required mixtures of the above solvents with DMF. The isolated complexes were characterized by matrix-assisted laser desorption/ionization time-of-flight mass spectrometry (MALDI-TOF MS). In all cases, the mass spectra showed an intense peak assigned to the hexametallate $[M_6^RL]^{+}$ ions and a series of signals originating from $[M_x^RL]^{+}$ ($x = 3, 4$) fragments (Figures 6 and S7–S12). As anticipated, these results are consistent with the formation of complexes of general formula $[M_2^RL]_3$. It is reasonable to assume that these complexes adopt molecular structures featuring two decks of M_3N_6 metallomacrocycles held together by the three clipping ferrocenyl spacers (Figure 7), similarly to the supramolecular structure of the protic proligand $[H_2^{MeL}]_3$ shown in Figure 2. This assumption is supported by the similarity of the mass spectra of the present series of complexes with those of the recently reported class of hexametallate complexes $[M_2^RL]_3$ with the closely related ferrocenyl/pyrazole hybrid ligands $[R^L]^{2-}$ (Figure 1), for which the solid-state structures could be authenticated by X-ray diffraction for two examples ($M = Cu^I$, $R = Me$ and $M = Ag^I$, $R = CF_3$).^[12] Unfortunately, all of the coinage-metal complexes of the new ligands $[R^L]^{2-}$ are practically insoluble in common organic solvents [such as acetone, CH_2Cl_2 , $CHCl_3$, MeOH, MeCN, $MeNO_2$, DMF, *N,N*-dimethylacetamide (DMA), and DMSO]; therefore, we have not yet obtained single crystals suitable for X-ray diffraction or studied the hexametallate

species in solution (by NMR spectroscopy and cyclic voltammetry). We tentatively attribute the insolubility to multiple intermolecular $d^{10}-d^{10}$ interactions that effectively lead to polymeric structures in the solid state, as was also observed for $[Cu_2^{MeL}]_3$.^[12]

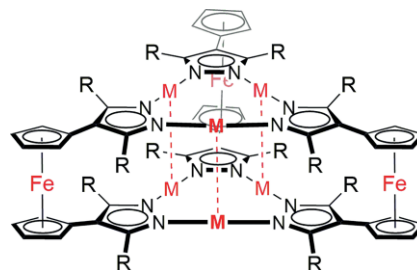


Figure 7. Proposed structure of $[M_2^RL]_3$ ($M = Cu^I$, Ag^I , Au^I ; $R = H$, Me).

The Mössbauer spectra of all $[M_2^RL]_3$ complexes are essentially identical to the spectra of the free proligands H_2^RL ; therefore, the electronic situation at the iron centers is not affected significantly when the appended pyrazole rings coordinate to monovalent coinage-metal ions. The Mössbauer parameters are compiled in Table 1.

As discussed in the Introduction, the luminescence properties of multinuclear coinage-metal pyrazolates are of particular interest and have been studied intensively.^[3,7a-7c,9a,10a] Therefore, preliminary investigations of the luminescence properties of the six new complexes were performed for solid (powder) samples. In all cases, upon excitation with UV light, a weak emission centered in the violet region of the visible spectrum was recorded (see the spectrum of $[Ag_2^HL]_3$ in Figure 8 as an example; the other spectra are shown in Figures S15–S19). Under the same conditions, the proligands themselves are weakly emitting at similar wavelengths (Figures S13 and S14). Thus, it is assumed that the transitions involved in the luminescence processes are mainly ligand-centered with only minor contributions from the coinage-metal ions and metallophilic $d^{10}-d^{10}$ interactions.

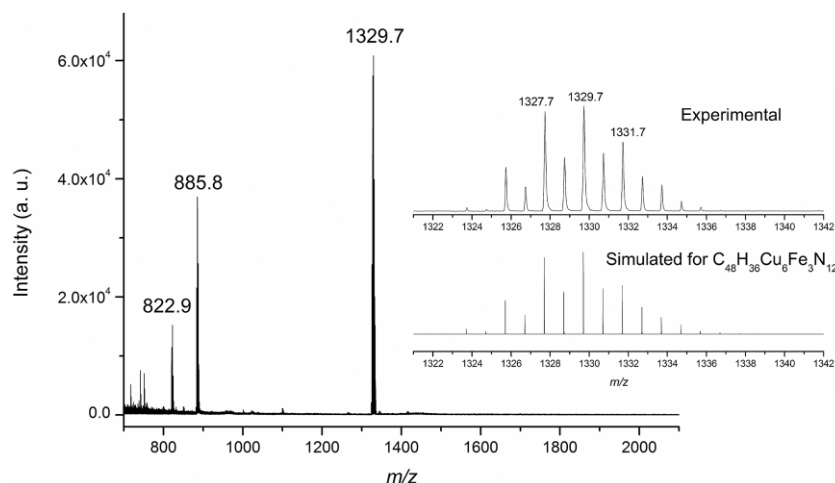


Figure 6. Positive-ion MALDI-TOF mass spectrum of $Cu_6^HL_3$ in DMF; the inset shows the experimental and simulated isotopic pattern for the molecular ion peak at $m/z = 1329.7$, which corresponds to $[Cu_6^HL_3]^+$. The peaks at $m/z = 822.9$ and 885.8 are assigned to ions $[Cu_3^HL_2]^+$ and $[Cu_4^HL_2]^+$, respectively.

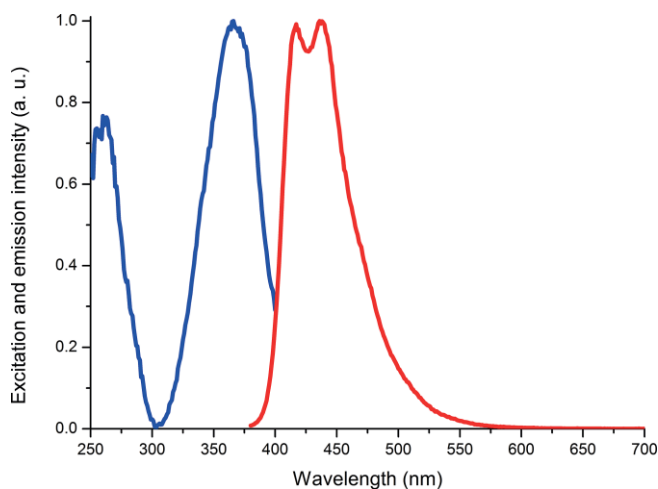


Figure 8. Photoluminescence spectra of $[\text{Ag}_2^{\text{HL}}]_3$. The emission spectrum (red) was recorded after excitation at $\lambda = 365$ nm, and the emission was monitored at $\lambda = 415$ nm for the excitation spectrum (blue).

Conclusions

In this work, we have successfully synthesized hybrid ferrocene/pyrazole molecules in which each of the ferrocene Cp rings is equipped with a pyrazole connected through its 4-position. In the solid state, H_2^{HL} and H_2^{MeL} form supramolecular aggregates, either dimeric $[\text{H}_2^{\text{HL}}]_2$ (C_2 symmetry) or trimeric $[\text{H}_2^{\text{MeL}}]_3$ (noncrystallographic D_3 symmetry), held together by intermolecular $\text{NH}\cdots\text{N}$ hydrogen bonds. For H_2^{MeL} , the trimers are also present in solution ($[\text{D}_8]$ toluene) at low temperature, whereas the aggregation of H_2^{HL} is likely prevented by the high polarity of the solvent ($[\text{D}_7]$ DMF) that is required to dissolve the compound. In their dianionic forms, H_2^{RL} serve as ligands towards monovalent Cu^I , Ag^I , and Au^I ions. On the basis of MALDI MS results and literature precedence for related systems, the complexes are proposed to have the general formula $[\text{M}_2^{\text{RL}}]_3$ and to be composed of two eclipsed decks of M_3N_6 metallomacrocycles linked by the three ferrocenyl moieties; such molecular structures would likely feature a prismatic arrangement of six coinage-metal ions and overall D_{3h} symmetry. Solution studies were hampered by the low solubilities of these $[\text{M}_2^{\text{RL}}]_3$ complexes. The substituents at the pyrazole rings (H or Me) exert the expected effects on the electrochemical redox potentials of the ferrocene moiety in the free proligands H_2^{HL} and H_2^{MeL} , and the ^{57}Fe Mössbauer parameters of all of the new compounds are insensitive to the identity of the pyrazole substituents R or the coinage-metal ions M and are similar to the Mössbauer parameters of the parent ferrocene itself. Unfortunately, on the basis of preliminary data, the luminescence properties of the solid compounds $[\text{M}_2^{\text{RL}}]_3$ ($\text{M} = \text{Cu}^I, \text{Ag}^I, \text{Au}^I$) are unremarkable, as was also observed for the related series of complexes $[\text{M}_2^{\text{RL}}]_3$.^[12]

The results presented in this article enlarge the still small family of 1,1'-bis(pyrazolyl)ferrocene molecules and delineate a promising strategy for the controlled stacking of pyrazole-based M_3N_6 metallomacrocycles. The introduction of pyrazole substituents other than H and Me (either more electron-withdrawing or bulkier) or the oxidation of the Fe^{II} centers could

lead to different electrochemical properties and to different supramolecular arrangements that could also prevent the intermolecular $d^{10}\text{-}d^{10}$ interactions that are likely responsible for the low solubilities of the compounds. On the other hand, metallocene linkers other than ferrocene could modulate the spacing of the two M_3N_6 decks. Studies in these directions are ongoing.

Experimental Section

General: The syntheses of proligands and Cu^I complexes were performed under an anaerobic and anhydrous atmosphere of dry argon by standard Schlenk techniques. Tetrahydrofuran (THF) was dried with sodium and potassium in the presence of benzophenone; MeOH, MeCN, and DMF were dried with CaH_2 ; hexane was dried with molecular sieves with an MBRAUN solvent purification system. NMR spectra were recorded with Bruker Avance 300 MHz and Bruker Avance 400 MHz spectrometers. Chemical shifts (δ) are reported in ppm and are referenced to the residual proton and carbon signals of the solvents (CDCl_3 : $\delta_{\text{H}} = 7.26$ ppm, $\delta_{\text{C}} = 77.16$ ppm; CD_2Cl_2 : $\delta_{\text{H}} = 5.32$ ppm, $\delta_{\text{C}} = 53.84$ ppm; $[\text{D}_6]$ DMSO: $\delta_{\text{H}} = 2.50$ ppm, $\delta_{\text{C}} = 39.52$ ppm; $[\text{D}_8]$ toluene: $\delta_{\text{H}} = 2.08$ ppm, $\delta_{\text{C}} = 20.43$ ppm; $[\text{D}_7]$ DMF: $\delta_{\text{H}} = 2.75$ ppm, $\delta_{\text{C}} = 29.76$ ppm). EI mass spectra were recorded with a Finnigan MAT 8200 instrument. MALDI-TOF mass spectra were recorded with a Bruker Autoflex Speed instrument. Cyclic voltammograms were measured with a PerkinElmer 263A potentiostat controlled by the Electrochemistry Powersuit software; a three-electrode arrangement was used with a glassy carbon working electrode, an $\text{Ag}/0.01$ M AgNO_3 reference electrode and a Pt wire counter electrode. All cyclic voltammograms were referenced externally to Fc/Fc^+ , for which the cyclic voltammogram of Fc was recorded under identical conditions immediately before or after the electrochemical experiments. The Mössbauer spectra were recorded with a ^{57}Co source in an Rh matrix with an alternating constant acceleration Wissel Mössbauer spectrometer operated in the transmission mode and equipped with a Janis closed-cycle helium cryostat. The isomer shifts are given relative to iron metal at ambient temperature. The simulation of the experimental data was performed with the Mfit program with Lorentzian line doublets.^[24] Elemental analyses were performed by the analytical laboratory of the Institute of Inorganic Chemistry at Georg August University with an Elementar Vario EL III instrument. 4-Iodo-1H-pyrazole was obtained from a commercial source (abcr GmbH), 4-iodo-3,5-dimethyl-1H-pyrazole was obtained either from a commercial source (abcr GmbH) or synthesized by an adapted literature procedure (see below).^[25] Details of the X-ray crystallographic structure determinations can be found in the Supporting Information. CCDC 1482525 (for H_2^{HL}), and 1482526 (for H_2^{MeL}) contain the supplementary crystallographic data for this paper. These data can be obtained free of charge from The Cambridge Crystallographic Data Centre.

4-Iodo-3,5-dimethyl-1H-pyrazole: 3,5-Dimethyl-1H-pyrazole (5.0 g, 52.0 mmol, 1.0 equiv.) was dissolved in H_2O (300 mL). I_2 (6.60 g, 26.0 mmol, 0.5 equiv.) and H_2O_2 (50 % aqueous solution, 1.8 mL, 31.7 mmol, 0.6 equiv.) were added, and the mixture was stirred at room temperature for 24 h. A precipitate formed and was separated by filtration, washed with H_2O (50 mL), and dissolved in CH_2Cl_2 . The organic solution was washed with a saturated aqueous solution of sodium thiosulfate to remove unreacted iodine and dried with MgSO_4 , and the solvent was removed under reduced pressure to give the title compound as a white solid (8.8 g, 39.6 mmol, 76 %). ^1H NMR (CDCl_3 , 300 MHz): $\delta = 2.26$ (s, 6 H, CH_3)

ppm. ^{13}C NMR (CDCl_3 , 75 MHz): $\delta = 13.1$ (CH_3), 62.7 (4-C^{Pz}), 146.7 ($3\text{-/}5\text{-C}^{\text{Pz}}$) ppm.

4-Iodo-1-(tetrahydropyran-2-yl)-1H-pyrazole ($^{\text{H}}$ I): 4-Iodo-1H-pyrazole (8.5 g, 43.8 mmol, 1.0 equiv.), 3,4-dihydro-2H-pyran (8 mL, 87.7 mmol, 2.0 equiv.), and *p*-toluenesulfonic acid (75 mg, 0.436 mmol, 0.01 equiv.) were dissolved in MeCN (20 mL), and the mixture was heated to reflux for 3 h. After cooling to room temperature, the solution was diluted with AcOEt (50 mL), washed with a saturated aqueous solution of NaHCO_3 , and dried with MgSO_4 . The solvent was then removed under reduced pressure to afford a dark brown oil. The crude material was purified by Kugelrohr distillation (110 °C, 5×10^{-3} mbar), and the product was obtained as a colorless oil (11.9 g, 42.8 mmol, 97 %). ^1H NMR (CDCl_3 , 300 MHz): $\delta = 1.59\text{--}1.73$ (m, 3 H), 1.99–2.10 (m, 3 H), 3.64–3.73 (m, 1 H), 4.00–4.07 (m, 1 H), 5.35–5.39 (m, 1 H), 7.54 (s, 1 H, 3- H^{Pz}), 7.66 (s, 1 H, 5- H^{Pz}) ppm. ^{13}C NMR (CDCl_3 , 75 MHz): $\delta = 22.3$ (5- C^{THP}), 25.0 (4- C^{THP}), 30.5 (6- C^{THP}), 57.3 (4- C^{Pz}), 67.8 (3- C^{THP}), 87.9 (1- C^{THP}), 132.4 (5- C^{Pz}), 144.6 (3- C^{Pz}) ppm.

4-Iodo-3,5-dimethyl-1-(tetrahydropyran-2-yl)-1H-pyrazole ($^{\text{MeI}}$): 4-Iodo-3,5-dimethyl-1H-pyrazole (7.5 g, 33.8 mmol, 1.0 equiv.), 3,4-dihydro-2H-pyran (6.2 mL, 68.0 mmol, 2.0 equiv.), and *p*-toluenesulfonic acid (58 mg, 0.34 mmol, 0.01 equiv.) were dissolved in MeCN (20 mL), and the mixture was heated to reflux for 3 h. After cooling to room temperature, the solution was diluted with AcOEt (50 mL), washed with a saturated aqueous solution of NaHCO_3 , and dried with MgSO_4 . The solvent was then removed under reduced pressure to afford a brownish solid. The crude material was washed with several small portions of cold MeOH (–40 °C) until a white powder resulted (6.51 g, 21.23 mmol, 63 %). More product was obtained by leaving the filtrate at –30 °C overnight (2.07 g, 6.76 mmol, 20 %). Overall yield: 8.58 g, 28.03 mmol, 83 %. ^1H NMR (CDCl_3 , 300 MHz): $\delta = 1.54\text{--}1.92$ (m, 3 H), 1.87–1.92 (m, 1 H), 2.23 (s, 3 H, CH_3), 2.33 (s, 3 H, CH_3), 2.07–2.10 (m, 1 H), 2.36–2.44 (m, 1 H), 3.59–3.66 (m, 1 H), 4.02–4.07 (m, 1 H), 5.22 (dd, $^3J_{\text{H,H}} = 10.2/2.4$ Hz, 1 H) ppm. ^{13}C NMR (CDCl_3 , 75 MHz): $\delta = 12.1$ (CH_3), 14.3 (CH_3), 23.0 (5- C^{THP}), 25.1 (4- C^{THP}), 29.5 (6- C^{THP}), 65.0 (4- C^{Pz}), 68.1 (3- C^{THP}), 85.4 (1- C^{THP}), 141.5 (5- C^{Pz}), 150.0 (3- C^{Pz}) ppm.

General Procedure for the Preparation of 1,1'-Bis(1H-pyrazol-4-yl)ferrocene ($\text{H}_2^{\text{H}}\text{L}$) and 1,1'-Bis(3,5-dimethyl-1H-pyrazol-4-yl)ferrocene ($\text{H}_2^{\text{MeI}}\text{L}$): *n*BuLi (1.6 M in hexane, 21 mL, 33.6 mmol, 2.1 equiv.) and TMEDA (5.1 mL, 34.0 mmol, 2.1 equiv.) were mixed in hexane (20 mL), and solid ferrocene (3.0 g, 16.1 mmol, 1.0 equiv.) was added after 15 min. The resulting solution was stirred overnight, and an orange suspension formed. The solvent was then removed under reduced pressure, and the residue was dissolved in THF (30 mL). The solution was cooled to 0 °C, and anhydrous ZnCl_2 (4.83 g, 35.4 mmol, 2.2 equiv.) was added in one portion. After 1 h of stirring, a solution containing the appropriate protected iodo-pyrazole (8.97 g, 32.3 mmol, 2.0 equiv. of $^{\text{H}}$ I for $\text{H}_2^{\text{H}}\text{L}$; 9.87 g, 32.2 mmol, 2.0 equiv. of $^{\text{MeI}}$ for $\text{H}_2^{\text{MeI}}\text{L}$) and Pd(PPh_3)₄ (900 mg, 5 mol-%) in THF (20 mL) was added to the reaction mixture. The resulting mixture was stirred at room temperature for 2.5 d, and then a saturated NaOH aqueous solution (100 mL) was added, and the layers were separated. The aqueous phase was extracted with CH_2Cl_2 (3×80 mL), the combined organic phases were dried with MgSO_4 , and the solvent was removed under reduced pressure. The crude material was purified by silica column chromatography with AcOEt as the eluent ($R_f = 0.49$ for $\text{H}_2^{\text{H}}\text{L}$ -THP; 0.53 for $\text{H}_2^{\text{MeI}}\text{L}$ -THP). The compound was deprotected by dissolving the THP derivate in MeOH (10 mL) and ethanolic HCl (10 mL) and stirring the solution overnight. For $\text{H}_2^{\text{H}}\text{L}$, the resulting suspension was neutralized with NaHCO_3 in water and filtered, and the resulting solid was dried in

vacuo; for $\text{H}_2^{\text{MeI}}\text{L}$, the solid was first collected by filtration, washed with NaHCO_3 (aq), and finally dried in vacuo.

$\text{H}_2^{\text{H}}\text{L}$: The product was obtained as an ochre powder (2.10 g, 6.6 mmol, 41 %). Crystals suitable for X-ray diffraction were obtained by vapor diffusion of EtOH into a solution of the compound in DMF. ^1H NMR ($[\text{D}_6]\text{DMSO}$, 300 MHz): $\delta = 4.02$ (t, $J = 1.8$ Hz, 4 H, 3-/4- H^{Fc}), 4.28 (t, $J = 1.8$ Hz, 4 H, 2-/5- H^{Fc}), 7.55 (s, 4 H, CH^{Pz}), 12.63 (br., 2 H, NH) ppm. ^{13}C NMR ($[\text{D}_6]\text{DMSO}$, 75 MHz): $\delta = 67.6$ (2-/5- C^{Fc}), 68.8 (3-/4- C^{Fc}), 79.3 (1- C^{Fc}), 117.3 (4- C^{Pz}), 130.7 (3-/5- C^{Pz}) ppm. ^1H NMR ($[\text{D}_7]\text{DMF}$, 300 MHz): $\delta = 4.06$ (s, 4 H, 3-/4- H^{Fc}), 4.37 (s, 4 H, 2-/5- H^{Fc}), 7.67 (s, 4 H, CH^{Pz}), 12.80 (s, 2 H, NH) ppm. MS (EI): m/z (%) = 318.0 (100) [$\text{M}]^+$. $\text{C}_{16}\text{H}_{14}\text{FeN}_4 \cdot 1/3\text{DMF}$ (342.5): calcd. C 59.61, H 4.81, N 17.72; found C 59.31, H 4.52, N 17.49.

$\text{H}_2^{\text{MeI}}\text{L}$: The product was obtained as an orange powder (1.94 g, 5.16 mmol, 32 %). Crystals suitable for X-ray diffraction were obtained by slow cooling of a hot solution of the compound in toluene. ^1H NMR ($[\text{D}_6]\text{DMSO}$, 300 MHz): $\delta = 2.19$ (s, 12 H, CH_3), 4.11 (s, 4 H, 3-/4- H^{Fc}), 4.26 (s, 4 H, 2-/5- H^{Fc}), 12.05 (br., 2 H, NH) ppm. ^{13}C NMR ($[\text{D}_6]\text{DMSO}$, 75 MHz): $\delta = 12.2$ (CH_3), 67.2 (2-/5- C^{Fc}), 68.3 (3-/4- C^{Fc}), 80.3 (1- C^{Fc}), 110.9 (4- C^{Pz}) ppm; the signal for 3-/5- C^{Pz} could not be detected. ^1H NMR (CDCl_3 , 300 MHz): $\delta = 2.29$ (s, 12 H, CH_3), 4.26 (s, 4 H, 3-/4- H^{Fc}), 4.48 (s, 4 H, 2-/5- H^{Fc}), 12.46 (br., 2 H, NH) ppm. ^1H NMR (CD_2Cl_2 , 400 MHz): $\delta = 2.28$ (s, 12 H, CH_3), 4.28 (s, 4 H, 3-/4- H^{Fc}), 4.52 (s, 4 H, 2-/5- H^{Fc}) ppm. ^1H NMR ($[\text{D}_3]\text{toluene}$, 400 MHz): $\delta = 2.16$ (s, 12 H, CH_3), 4.09 (s, 4 H, 3-/4- H^{Fc}), 4.26 (s, 4 H, 2-/5- H^{Fc}) ppm. ^1H NMR ($[\text{D}_7]\text{DMF}$, 400 MHz): $\delta = 2.30$ (s, 12 H, CH_3), 4.16 (t, $J = 2$ Hz, 4 H, 3-/4- H^{Fc}), 4.36 (t, $J = 2$ Hz, 4 H, 2-/5- H^{Fc}), 12.14 (br., 2 H, NH) ppm. MS (EI): m/z (%) = 474.1 (100) [$\text{M}]^+$. $\text{C}_{20}\text{H}_{22}\text{FeN}_4 \cdot 1/7\text{toluene}$ (387.4): calcd. C 65.10, H 6.02, N 14.46; found C 64.79, H 6.28, N 14.21.

General Procedure for the Preparation of the Copper Complexes: The appropriate proligand $\text{H}_2^{\text{R}}\text{L}$ (1.0 equiv.) and $[\text{Cu}(\text{MeCN})_4][\text{BF}_4]$ (2.0 equiv.) were dissolved in dry MeOH (5 mL for $\text{H}_2^{\text{MeI}}\text{L}$) or MeOH/DMF (3:1; 12 mL for $\text{H}_2^{\text{H}}\text{L}$). After 3 min, degassed Et_3N (0.1 mL) was added dropwise, and a suspension formed immediately. The reaction mixture was stirred for 2 h. The resulting solid was separated by filtration, washed with MeOH, and dried in vacuo. Owing to the insolubility of the products in any solvent, single-crystalline material of analytical purity could not be obtained.

$[\text{Cu}_2^{\text{H}}\text{L}]_3$: 1.0 equiv., 0.314 mmol. The product was obtained as a dark green solid (117 mg, 0.088 mmol, 84 %). MS (MALDI-TOF): m/z (%) = 822.9 (30) [Cu_3L_2] $^+$, 885.8 (65) [Cu_4L_2] $^+$, 1329.7 (100) [Cu_6L_3] $^+$.

$[\text{Cu}_2^{\text{MeI}}\text{L}]_3$: 1.0 equiv., 0.198 mmol. The product was obtained as an orange-brown solid (82 mg, 0.0547 mmol, 83 %). ^1H NMR (CDCl_3 , 400 MHz): $\delta = 2.19$ (s, 12 H, CH_3), 4.27 (s, 4 H, 3-/4- H^{Fc}), 4.41 (s, 4 H, 2-/5- H^{Fc}) ppm. ^1H NMR ($[\text{D}_7]\text{DMF}$, 300 MHz): $\delta = 2.07$ (s, 12 H, CH_3), 4.67 (s, 4 H, 3-/4- H^{Fc}), 4.81 (s, 4 H, 2-/5- H^{Fc}) ppm. MS (MALDI-TOF): m/z (%) = 935.0 (24) [$\text{Cu}_3\text{L}_2 + \text{H}$] $^+$, 998.0 (100) [Cu_4L_2] $^+$, 1497.9 (35) [Cu_6L_3] $^+$.

General Procedure for the Preparation of the Silver Complexes: The appropriate proligand $\text{H}_2^{\text{R}}\text{L}$ (1.0 equiv.) was dissolved in MeCN (10 mL for $\text{H}_2^{\text{MeI}}\text{L}$) or MeCN/DMF (3:1; 20 mL for $\text{H}_2^{\text{H}}\text{L}$), and a solution of AgBF_4 (2.0 equiv.) in MeCN (2 mL) was added. After 3 min, Et_3N (0.1 mL) was added dropwise, and a precipitate formed immediately. The mixture was stirred for 1 h, and then the solid was separated by filtration, washed with MeCN and MeOH, and dried in vacuo.

$[\text{Ag}_2^{\text{H}}\text{L}]_3$: 1.0 equiv., 0.261 mmol. The product was obtained as an orange/red solid (107 mg, 0.067 mmol, 72 %). MS (MALDI-TOF): m/z (%) = 741.6 (86), 769.6 (100), 818.4 (83), 955.9 (60) [$\text{Ag}_3\text{L}_2 + \text{H}$] $^+$, 1063.8 (53) [Ag_4L_2] $^+$, 1100.9 (70), 1595.7 (73) [Ag_6L_3] $^+$.

$C_{48}H_{36}Ag_6Fe_3N_{12} \cdot DMF$ (1668.7): calcd. C 36.71, H 2.60, N 10.91; found C 37.35, H 2.71, N 10.45.

[Ag^{Me}L₃]: 1.0 equiv., 0.222 mmol. The product was obtained as a dark red solid (102 mg, 0.058 mmol, 78 %). MS (MALDI-TOF): *m/z* (%) = 672.6 (100), 1068.0 (11) [Ag₃L₂ + H]⁺, 1175.9 (22) [Ag₄L₂]⁺, 1763.8 (66) [Ag₆L₃]⁺. $C_{60}H_{60}Ag_6Fe_3N_{12}$ (1763.96): calcd. C 40.85, H 3.43, N 9.53; found C 40.71, H 3.59, N 8.84.

General Procedure for the Preparation of the Gold Complexes: The appropriate proligand H₂^RL (1.0 equiv.) and AuCl(SMe₂) (2.0 equiv.) were mixed in MeCN (10 mL for H₂^{Me}L) or MeCN/DMF (3:1; 10 mL for H₂^HL). After the addition of Et₃N (0.1 mL), the reaction mixture was stirred overnight. The resulting solid was then separated by filtration, washed with MeCN and THF, and dried in vacuo. Owing to the insolubility of the products in any solvent, single-crystalline material of analytical purity could not be obtained.

[Au₂^HL₃]: 1.0 equiv., 0.088 mmol. The product was obtained as a green solid (52 mg, 0.024 mmol, 82 %). MS (MALDI-TOF): *m/z* (%) = 2130.0 (100) [Au₆L₃]⁺.

[Au₂^{Me}L₃]: 1.0 equiv., 0.142 mmol. The product was obtained as a brown solid (100 mg, 0.0435 mmol, 92 %). MS (MALDI-TOF): *m/z* (%) = 1336.1 (12) [Au₃L₂]⁺, 1532.1 (100) [Au₄L₂]⁺, 1907.2 (13) [Au₄L₃ + 3H]⁺, 2102.2 (30) [Au₅L₃ + H]⁺, 2298.1 (31) [Au₆L₃]⁺.

Acknowledgments

Financial support by the Georg-August-Universität Göttingen is gratefully acknowledged.

Keywords: Coinage metals · Nitrogen heterocycles · Metallocenes · Oligonuclear complexes · Supramolecular chemistry

- [1] a) G. La Monica, G. A. Ardizzoia, *Prog. Inorg. Chem.* **1997**, *46*, 151–238; b) M. A. Halcrow, *Dalton Trans.* **2009**, 2059–2073; c) A. A. Mohamed, *Coord. Chem. Rev.* **2010**, *254*, 1918–1947.
- [2] N. Masciocchi, M. Moret, P. Cairati, A. Sironi, G. A. Ardizzoia, G. La Monica, *J. Am. Chem. Soc.* **1994**, *116*, 7668–7676.
- [3] K. Fujisawa, Y. Ishikawa, Y. Miyashita, K.-i. Okamoto, *Inorg. Chim. Acta* **2010**, *363*, 2977–2989.
- [4] a) H. H. Murray, R. G. Raptis, J. P. Fackler, *Inorg. Chem.* **1988**, *27*, 26–33; b) G. A. Ardizzoia, S. Cenini, G. La Monica, N. Masciocchi, M. Moret, *Inorg. Chem.* **1994**, *33*, 1458–1463; c) G. Yang, R. G. Raptis, *Inorg. Chim. Acta* **2003**, *352*, 98–104; d) A. Maspero, S. Brenna, S. Galli, A. Penoni, *J. Organomet. Chem.* **2003**, *672*, 123–129.
- [5] a) R. G. Raptis, J. P. Fackler, *Inorg. Chem.* **1988**, *27*, 4179–4182; b) R. G. Raptis, H. H. Murray, J. P. Fackler, *J. Chem. Soc., Chem. Commun.* **1987**, 737–739.
- [6] C.-Y. Zhang, J.-B. Feng, Q. Gao, Y.-B. Xie, *Acta Crystallogr., Sect. E* **2008**, *64*, m352.
- [7] a) H. V. R. Dias, H. V. K. Diyabalanage, M. A. Rawashdeh-Omary, M. A. Franzman, M. A. Omary, *J. Am. Chem. Soc.* **2003**, *125*, 12072–12073; b) H. V. R. Dias, H. V. K. Diyabalanage, M. G. Eldabaja, O. Elbjeirami, M. A. Rawashdeh-Omary, M. A. Omary, *J. Am. Chem. Soc.* **2005**, *127*, 7489–7501; c) M. A. Omary, M. A. Rawashdeh-Omary, M. W. A. Gonser, O. Elbjeirami, T. Grimes, T. R. Cundari, H. V. K. Diyabalanage, C. S. P. Gamage, H. V. R. Dias, *Inorg. Chem.* **2005**, *44*, 8200–8210; d) H. V. R. Dias, C. S. P. Gamage, J. Keltner, H. V. K. Diyabalanage, I. Omari, Y. Eyobo, N. R. Dias, N. Roehr, L. McKinney, T. Poth, *Inorg. Chem.* **2007**, *46*, 2979–2987.
- [8] a) H. V. Rasika Dias, C. S. P. Gamage, *Angew. Chem. Int. Ed.* **2007**, *46*, 2192–2194; *Angew. Chem.* **2007**, *119*, 2242; b) M. A. Omary, O. Elbjeirami, C. S. P. Gamage, K. M. Sherman, H. V. R. Dias, *Inorg. Chem.* **2009**, *48*, 1784–1786; c) N. B. Jayaratna, C. V. Hettiarachchi, M. Yousufuddin, H. V. Rasika Dias, *New J. Chem.* **2015**, *39*, 5092–5095.
- [9] a) A. Kishimura, T. Yamashita, T. Aida, *J. Am. Chem. Soc.* **2005**, *127*, 179–183; b) T. Osuga, T. Murase, M. Fujita, *Angew. Chem. Int. Ed.* **2012**, *51*, 12199–12201; *Angew. Chem.* **2012**, *124*, 12365; c) W.-X. Ni, Y.-M. Qiu, M. Li, J. Zheng, R. W.-Y. Sun, S.-Z. Zhan, S. W. Ng, D. Li, *J. Am. Chem. Soc.* **2014**, *136*, 9532–9535.
- [10] a) C. V. Hettiarachchi, M. A. Rawashdeh-Omary, D. Korir, J. Kohistani, M. Yousufuddin, H. V. R. Dias, *Inorg. Chem.* **2013**, *52*, 13576–13583; b) T. Grimes, M. A. Omary, H. V. R. Dias, T. R. Cundari, *J. Phys. Chem. A* **2006**, *110*, 5823–5830.
- [11] a) T. Jozak, Y. Sun, Y. Schmitt, S. Lebedkin, M. Kappes, M. Gerhards, W. R. Thiel, *Chem. Eur. J.* **2011**, *17*, 3384–3389; b) G.-F. Gao, M. Li, S.-Z. Zhan, Z. Lv, G.-h. Chen, D. Li, *Chem. Eur. J.* **2011**, *17*, 4113–4117; c) A. C. Jahnke, K. Pröpper, C. Bronner, J. Teichgräber, S. Dechert, M. John, O. S. Wenger, F. Meyer, *J. Am. Chem. Soc.* **2012**, *134*, 2938–2941; d) M. Veronelli, N. Kindermann, S. Dechert, S. Meyer, F. Meyer, *Inorg. Chem.* **2014**, *53*, 2333–2341; e) M. Veronelli, N. Kindermann, S. Dechert, F. Meyer, *J. Indian Chem. Soc.* **2015**, *92*, 1973–1980.
- [12] M. Veronelli, S. Dechert, S. Demeshko, F. Meyer, *Inorg. Chem.* **2015**, *54*, 6917–6927.
- [13] R. Horikoshi, *Coord. Chem. Rev.* **2013**, *257*, 621–637.
- [14] a) D. Braga, M. Polito, M. Braccini, D. D'Addario, E. Tagliavini, L. Sturba, F. Grepioni, *Organometallics* **2003**, *22*, 2142–2150; b) R. Horikoshi, C. Nambu, T. Mochida, *New J. Chem.* **2004**, *28*, 26–33; c) T. Mochida, F. Shimizu, H. Shimizu, K. Okazawa, F. Sato, D. Kuwahara, *J. Organomet. Chem.* **2007**, *692*, 1834–1844.
- [15] a) C. R. Hauser, C. E. Cain, *J. Org. Chem.* **1958**, *23*, 1142–1146; b) C. E. Cain, T. A. Mashburn, C. R. Hauser, *J. Org. Chem.* **1961**, *26*, 1030–1034; c) K. Schlögl, H. Egger, *Monatsh. Chem.* **1963**, *94*, 1054–1063; d) W. R. Thiel, T. Priemeier, D. A. Fiedler, A. M. Bond, M. R. Mattner, *J. Organomet. Chem.* **1996**, *514*, 137–147; e) G. K. Verma, R. K. Verma, M. S. Singh, *RSC Adv.* **2013**, *3*, 245–252.
- [16] a) S. Tampier, S. M. Bleifuss, M. M. Abd-Elzاهر, J. Sutter, F. W. Heinemann, N. Burzlaff, *Organometallics* **2013**, *32*, 5935–5945; b) K. Mohanan, A. R. Martin, L. Toupet, M. Smietana, J.-J. Vasseur, *Angew. Chem. Int. Ed.* **2010**, *49*, 3196–3199; *Angew. Chem.* **2010**, *122*, 3264.
- [17] a) J. L. G. de Paz, J. Elguero, C. Foces-Foces, A. L. Llamas-Saiz, F. Aguilarr-Parrilla, O. Klein, H.-H. Limbach, *J. Chem. Soc. Perkin Trans. 2* **1997**, 101–110; b) R. M. Claramunt, C. López, M. D. Santa María, D. Sanz, J. Elguero, *Prog. Nuc. Magn. Reson. Spectrosc.* **2006**, *49*, 169–206; c) H. V. R. Dias, H. V. K. Diyabalanage, *Polyhedron* **2006**, *25*, 1655–1661.
- [18] J. Sandström, *Dynamic NMR Spectroscopy*, Academic Press, London, **1982**.
- [19] M. T. Chenon, C. Coupry, D. M. Grant, R. J. Pugmire, *J. Org. Chem.* **1977**, *42*, 659–661.
- [20] W. M. Litchman, *J. Am. Chem. Soc.* **1979**, *101*, 545–547.
- [21] A. R. Katritzky, *Handbook of Heterocyclic Chemistry*, Elsevier Science, Oxford, **2013**.
- [22] M. Watanabe, H. Sano, *Bull. Chem. Soc. Jpn.* **1990**, *63*, 777–784.
- [23] N. G. Connelly, W. E. Geiger, *Chem. Rev.* **1996**, *96*, 877–910.
- [24] E. Bill, *Mfit*, Max-Planck Institute for Chemical Energy Conversion, Mülheim an der Ruhr, **2008**.
- [25] M. M. Kim, R. T. Ruck, D. Zhao, M. A. Huffman, *Tetrahedron Lett.* **2008**, *49*, 4026–4028.

Received: May 31, 2016

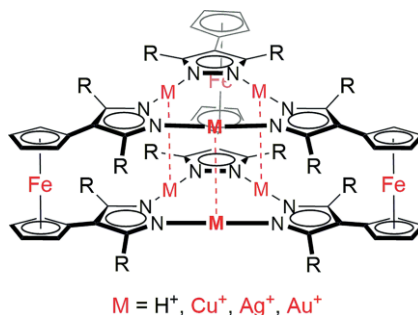
Published Online: ■

Ferrocenyl Ligands

M. Veronelli, S. Dechert,
A. Schober, S. Demeshko,
F. Meyer* 1–9



1,1'-Bis(pyrazol-4-yl)ferrocenes: Potential Clip Ligands and Their Supramolecular Structures



Supramolecular double deckers of the common pyrazolate-based $[M(\mu\text{-pz})_3]$ metallomacrocycles ($M = Cu^I, Ag^I, Au^I$; pz = pyrazolate) are assembled from ferrocene derivatives with two C-4-appended pyrazole rings. The ferrocene/pyrazole proligands $H_2^R L$ form dimeric or trimeric supramolecular aggregates through intermolecular $NH\cdots N$ hydrogen bonds, both in the solid state and in solution.

DOI: 10.1002/ejic.201600644